

# Syntheses and structural characterizations of 24-membered dimetal (Mn, Ni, Fe) macrocyclic complexes and the C–S bond formation between acetylacetonate and a mercapto N-heterocycle†‡

Xiaofeng Zhang, Hui Chen, Chengbing Ma, Changneng Chen and Qiutian Liu\*

Received 29th March 2006, Accepted 31st May 2006

First published as an Advance Article on the web 14th June 2006

DOI: 10.1039/b604579k

An organic ligand 2,5-di(3-pentanedionylthio)-1,3,4-thiadiazole ( $H_2L$ ) reacts with metal (Mn, Ni, Fe) salts, resulting in 24-membered dimetal macrocyclic complexes  $[MnL(H_2O)(dmsO)]_2 \cdot 2dmsO$  (**1**),  $[NiL(H_2O)(dmf)]_2 \cdot 2dmf$  (**2**),  $[MnL(dmf)_2]_2$  (**3**) and  $[Fe_2L_2(solvent)_2(SO_4)]$  (solvent = dmsO (**6**);  $H_2O$  (**7**); dmf (**8**)). Di-manganese macrocyclic complexes  $[MnL(dmf)(dmsO)]_2$  (**4**) and  $[MnL(H_2O)_2]_2 \cdot 6H_2O$  (**5**) can also be obtained directly by aerobic assembly reaction of  $MnCl_2$ , dipotassium 1,3,4-thiadiazole-2,5-dithiolate ( $K_2tdadt$ ) and acetylacetonate ( $H_2acac$ ) in various solvents, accompanying a C–S bond formation between acetylacetonate and the mercapto N-heterocycle. Disulfide has been considered as the intermediate in the assembly reaction. Meanwhile an assembly reaction including  $MnCl_2$ , 2-mercaptobenzimidazole and  $H_2acac$  has produced an organic compound 2-(3-pentanedionylthio)benzimidazole with a new C–S bond. These dimetal complexes have similar macrocyclic structures, in which solvent molecules and sulfate coordinate to the octahedral metal in *trans*-configuration, whereas a pair of water molecules are located in octahedral *cis*-positions for **5** owing to a small steric effect. A host cavity of sufficiently large size exists in the macrocyclic structure to trap the solvent molecules and the sulfate anion. The IR spectra have been used to assign the solvent molecules trapped and the sulfate anion which is shown as a bridged bidentate ligand. Thermal analyses show the stability of the macrocyclic backbone below 200 °C and gradual release processes of the trapped solvent molecules. Decomposition and oxidation of the dimetal macrocycle backbone occur at 300–500 °C, resulting in a metal sulfate. Further decomposition led to metal oxide at 500–600 °C.

## Introduction

The assembly of metallamacrocyclic complexes has become an area of particular interest since the appealing structures of the metallamacrocycles can act as highly specific hosts used for selective recognition<sup>1</sup> of neutral molecules, cations and anions. Metallamacrocycles have also been reported to have diverse possible applications in switchable electron-transfer,<sup>2</sup> catalysis<sup>3</sup> and magnetism.<sup>4</sup> Some important review articles<sup>5</sup> have discoursed at great length on the self-assembly of metallamacrocycles. Polydentate bridging ligands<sup>1–14</sup> are generally used as a spacer to combine polyhedral metal nodes forming the metallamacrocyclic. Many interesting synthetic designs have been performed.<sup>10,13,14</sup> Among the metallamacrocyclic complexes, dimetal macrocyclic complexes have attracted great interest in recent years and become an important type of metallamacrocycles,<sup>15,16</sup> of which  $\beta$ -diketonate-based ligands as one of the organic spacers have been used.<sup>16</sup> Here, we report a novel bridging ligand 2,5-di(3-

pentanedionylthio)-1,3,4-thiadiazole ( $H_2L$ ), which has been used to prepare a series of 24-membered dimetal macrocyclic complexes in this work. This work also reports a C–S bond formation between acetylacetonate and a mercapto N-heterocycle leading to dimanganese 24-membered macrocyclic complexes.

## Results and discussion

### Synthesis

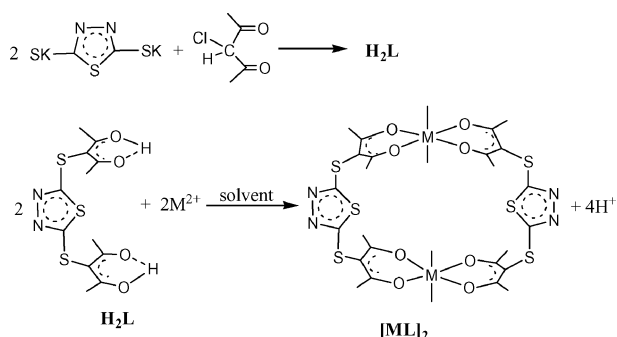
The ligand 2,5-di(3-pentanedionylthio)-1,3,4-thiadiazole ( $H_2L$ ) has been synthesized by reaction of  $ClHacac$  with dipotassium 2,5-dimercapto-1,3,4-thiadiazole in high yield. Two  $\beta$ -diketonate units existing in both sides of this molecule afford a possibility to chelate a pair of metal ions, constructing a macrocyclic dimetallic complex  $[ML]_2$  as shown in Scheme 1.

The dimetal 24-membered macrocyclic complexes synthesized were as follows:  $[MnL(H_2O)(dmsO)]_2 \cdot 2dmsO$  (**1**),  $[NiL(H_2O)(dmf)]_2 \cdot 2dmf$  (**2**),  $[MnL(dmf)_2]_2$  (**3**),  $[MnL(dmf)(dmsO)]_2$  (**4**),  $[MnL(H_2O)_2]_2 \cdot 6H_2O$  (**5**),  $[Fe_2L_2(dmsO)_2(SO_4)] \cdot 2H_2O$  (**6**),  $[Fe_2L_2(H_2O)_2(SO_4)] \cdot 2H_2O$  (**7**) and  $[Fe_2L_2(dmf)_2(SO_4)] \cdot 2CH_2Cl_2$  (**8**).

Metal salts,  $Mn(OAc)_2$ ,  $Ni(NO_3)_2$  and  $FeSO_4$  react with  $H_2L$  resulting in 24-membered dimetal (Mn, Ni, Fe) macrocyclic complexes. The reaction of  $FeSO_4$  with  $H_2L$  only resulted in di-Fe(III) macrocycle complexes **6**, **7** and **8**, showing the oxidation from Fe(II) to Fe(III). It is noted that the di-Mn macrocycles, such as **4** and **5**, can also be prepared from an assembly reaction of

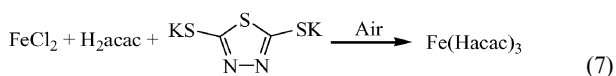
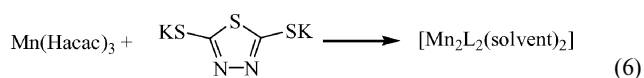
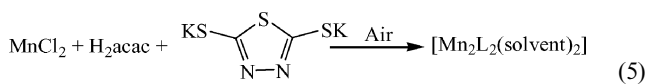
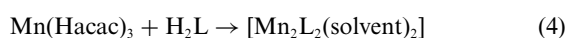
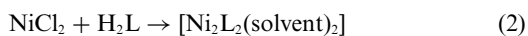
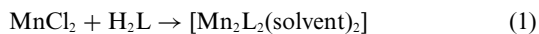
State Key Laboratory of Structural Chemistry, Fujian Institute of Research on the Structure of Matter, Chinese Academy of Sciences, Fuzhou, Fujian, 350002, China. E-mail: lqt@ms.fjirsm.ac.cn

† The HTML version of this article has been enhanced with colour images.  
‡ Electronic supplementary information (ESI) available: Fig. S1: packing diagram of  $H_2L$ ; Fig. S2–S4: structure and packing diagram of **1**·2dmsO; Fig. S5 and S6: structure and packing diagram of **4**; Fig. S7: rough structure of **7**; Fig. S8–S14: DTA and TG curves determined for  $H_2L$ , **2**, **4** and **5** under dinitrogen or air atmosphere; and the data of IR spectra for all the complexes. See DOI: 10.1039/b604579k



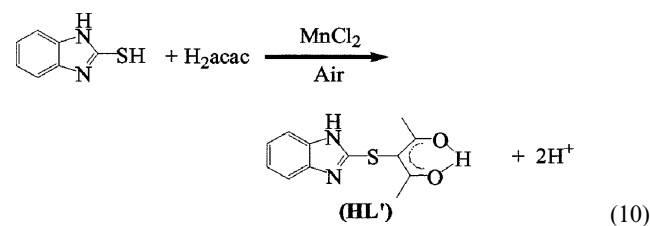
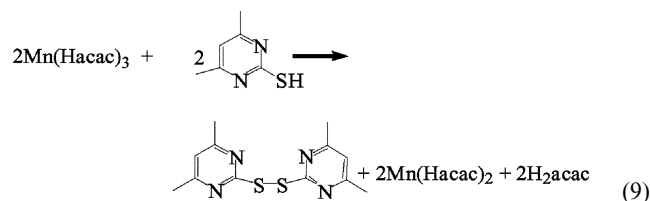
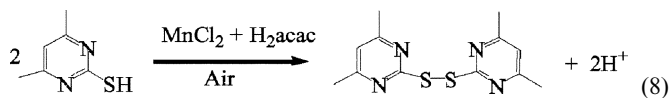
**Scheme 1** Dimetal 24-membered macrocyclic complexes were obtained from the reaction of a metal(II) salt (metal = Mn, Ni, Fe) with  $H_2L$ .

the precursors  $H_2acac$ ,  $K_2tdadt$  and  $MnCl_2 \cdot 4H_2O$ . The reaction of  $Mn(Hacac)_3$  with  $K_2tdadt$  has also led to the di-Mn(II) macrocycle **3**. Obviously, C–H bond activation of  $H_2acac$  accompanied with C–S bond formation between  $H_2acac$  and the  $tdadt$  anion has occurred in the assembly reaction. Related reactions are shown as follows:



of which, eqn (1)–(4) represent the reactions of metal salt with  $H_2L$  to give Mn(II), Ni(II) and Fe(III) macrocycles, while eqn (5) and (6) indicate the C–S bond fusion accompanying the formation of the Mn(II) macrocycles in the assembly reaction. However, similar assembly reaction of ferrous or ferric chloride only led to the formation of  $Fe(Hacac)_3$  (eqn (7)) under aerobic conditions and further C–S bond fusion between  $H_2acac$  and  $tdadt$  anion had not been found. Other assembly reactions with Ni, Co and Cu salts have not yet produced separable products. Therefore, the participation of Mn salts is considered to be essential for the formation of the C–S bond in preparing **4** and **5**. C–H bond activation accompanying with C–S bond formation is attractive in organometallic chemistry. Researches<sup>17,18</sup> have mentioned the catalysis of Mn ion and disulfide as a possible intermediate. Metal acetylacetonates have an activable C–H bond and can be expected to easily react with S-electrophiles, forming C–S bonds. As reported in the literature Mn(III) complexes can be obtained from Mn(II) reactants by aerial oxidation,<sup>19</sup> while the Mn(III) ion is reduced in oxidation of thiolate to get a disulfide

intermediate.<sup>20</sup> An early example reported the C–S bond formation between a metal acetylacetonate and a disulfide (thiocyanogen),<sup>21</sup> while preparation of  $2-C_5H_4N(acac-S)Pd(Hacac)$  is a recent example of C–S bond formation between disulfide and palladium acetylacetonate.<sup>22</sup> The disulfide is therefore proposed as an intermediate in the assembly of the di-Mn macrocycles. It is noted that the standard potential (1.51 V) of  $Mn^{III}/Mn^{II}$  is obviously higher than that (0.77 V) of  $Fe^{III}/Fe^{II}$ , implying that  $Mn^{III}$  has stronger ability to oxidize the sulfide to give the disulfide. Such considerations may also explain why Fe(III) is unable to induce the assembly of dimetal macrocycles in the same way as Mn(III) species do. The Mn(III) species can oxidize the thiolate to form the disulfide with concomitant reduction of Mn(III) to Mn(II) and then the Mn(II) species is aerobically reoxidised. The aerial oxidation of the Mn(II) is necessary for the synthesis of dimanganese macrocycle **5**. A parallel anaerobic assembly reaction using  $MnCl_2 \cdot 4H_2O$  was performed and did not lead to any separable product from the reaction solution during a long period (two months). However, the di-Mn macrocyclic complex **5** was rapidly produced when exposing the reaction solution to air (see Experimental section). Compared to Mn(II), the reaction starting from  $Mn^{III}(Hacac)_3$  successfully afforded **5** (Experimental section, method 2). These experiments indicate that the  $Mn(II) \rightarrow Mn(III)$  oxidation is important for the formation of the di-Mn macrocycle. When 4,6-dimethyl-2-mercaptopyrimidine reacts with  $MnCl_2 \cdot 4H_2O$  and  $H_2acac$  under aerobic conditions, a disulfide bis-(4,6-dimethylpyrimidine) 2,2'-disulfide was obtained in 42.5% yield and was identified by X-ray diffraction,<sup>23</sup> indicating the existence of the disulfide as an intermediate. Meanwhile, the disulfide can be also obtained in 77.9% yield by the oxidation of 4,6-dimethyl-2-mercaptopyrimidine in the presence of  $Mn(Hacac)_3$ . However, eqn (8) and (9) show no evidence for the further product of C–S bond fusion, implying the limitation of the disulfide for further reaction. Even so, a successful C–S bond formation between  $H_2acac$  and 2-mercaptobenzimidazole in the presence of  $MnCl_2$  under aerobic conditions has been performed (eqn (10)) accompanying the formation of an organic compound  $HL'$ .



## Structures

**H<sub>2</sub>L.** The structure of H<sub>2</sub>L shown in Fig. 1 contains two enolic six-membered rings at each end of the molecule. A pseudo-C<sub>2</sub> axis passes through S2 and the middle of the N1–N2 bond. Eight non-hydrogen atoms (5C + 2O + 1S) in the Hacac–S unit are coplanar with a largest deviation of 0.0202 Å from the least square plane. The dihedral angles between the Hacac–S and the 1,3,4-thiadiazole planes are 83.7 and 85.9°, which are connected by C6–S1–C3 and C7–S3–C10A to form a cambered molecule. Intermolecular hydrogen-bonding interaction was not found in the packing diagram (ESI, Fig. S1†), in which neighboring 1,3,4-thiadiazole rings align parallel along the *b* axis. The closest distance between the thiadiazole planes is 3.4074 Å, indicating face to face π–π stacking interactions.<sup>24</sup>

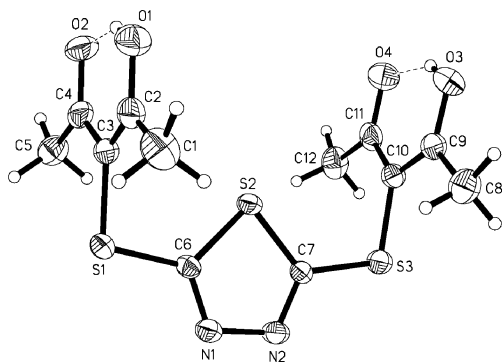


**Fig. 1** An enolic structure of 2,5-di(3-pentanedionylthio)-1,3,4-thiadiazole (H<sub>2</sub>L) with independent atom-labeling showing thermal ellipsoids at 30% probability.

**24-Membered dimetal macrocyclic complexes.** Complexes 1–4 with a common formula [ML(solvent)<sub>2</sub>]<sub>2</sub> have similar dimetal macrocyclic structures shown in Fig. 2–4 (see also Fig. S2–S6, ESI†). A crystallographically imposed symmetrical center exists within each the macrocycle. Eight non-hydrogen atoms (5C + 2O + 1S) in each the acac-S units are coplanar with deviation of 0.025–0.0633 Å from the least square plane. The metal ion is chelated by the acac groups forming two non-planar six-membered

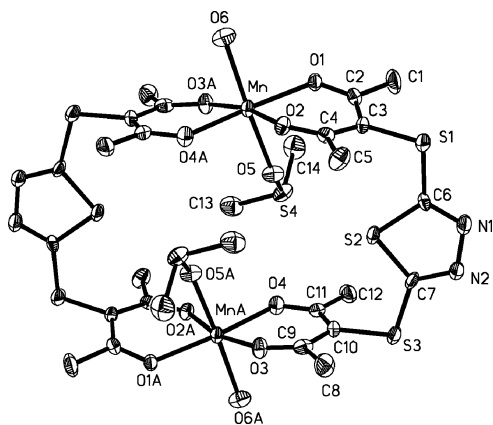


**Fig. 2** Structure of 1 showing thermal ellipsoids at 30% probability. Two dmso ligands extend to the inner space of the macrocycle. The other two solvate dmso molecules lying outside the macrocycle are omitted for simplify (symmetry code: A:  $-x + 2, -y + 2, -z + 2$ ).

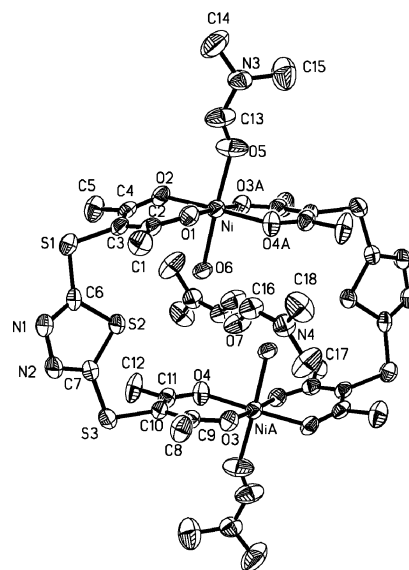


**Fig. 3** Structure of 2 showing thermal ellipsoids at 30% probability. Two dmso ligands extend to the inner space of the macrocycle (symmetry code: A:  $-x + 2, -y + 2, -z + 2$ ).

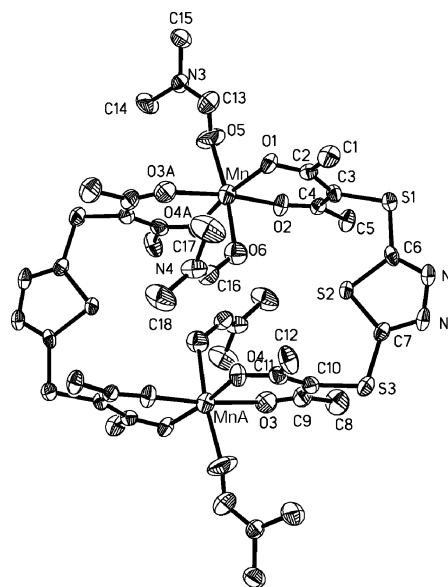


**Fig. 4** Structure of 3 with two dmf ligands at opposed positions in the coordination sphere of the Mn ion showing thermal ellipsoids at 30% probability (symmetry code: A:  $-x + 1, -y + 2, -z + 1$ ).

chelating rings. The acac oxygen atoms occupy the equatorial plane of the octahedral metal with rather small dihedral angles between the O1–M–O2 and O3A–M–O4A planes (1, 5.5°, 2, 3.0°, 3, 2.2° and 4, 5.8°). The dihedral angles between the thiadiazole ring and the acac-S planes are 94.2, 104.6° for 1; 84.3, 83.1° for 2; 80.3, 82.6° for 3 and 97.7, 100.5° for 4, which are fairly similar to those of the free ligand. It is worthwhile to notice that both the thiadiazole ring planes in these complexes are exactly parallel.

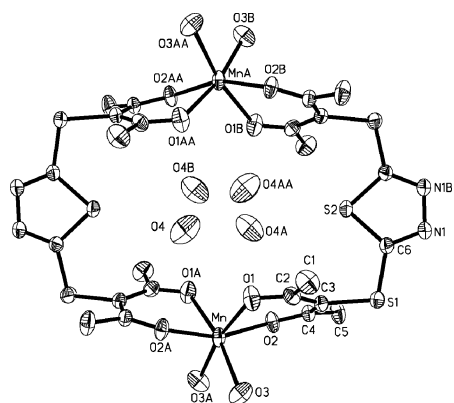
Two solvent ligands are located at opposed positions with a solvent molecule extending to the inner space of the macrocycle. Selected bond distances and angles and other comparable structural parameters for all 24-membered dimetal macrocyclic complexes in this work are listed in Table 1.

**Table 1** Summary of selected bond distances (Å) and angles (°) together with other structural parameters for 24-membered dimetal macrocyclic complexes

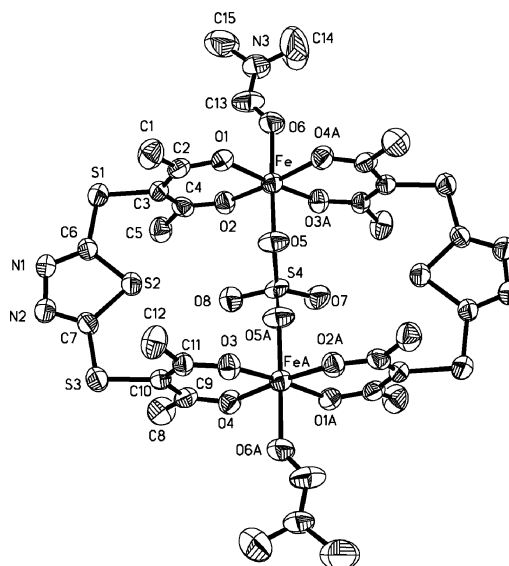
Compound	1	2	3	4	5	8
M–O1	2.121(6)	2.009(5)	2.138(4)	2.112(4)	2.138(3)	1.968(6)
M–O2	2.135(6)	2.009(5)	2.121(3)	2.137(4)	2.135(3)	1.972(7)
M–O3A	2.113(6)	1.995(5)	2.133(4)	2.133(4)	2.158(4) (H <sub>2</sub> O) <sup>a</sup>	1.986(6)
M–O4A	2.121(6)	1.998(5)	2.134(4)	2.146(4)		1.967(6)
M–O5	2.197(7) (dmsol) <sup>a</sup>	2.045(7) (dmf) <sup>a</sup>	2.150(5) (dmf) <sup>a</sup>	2.189(5) (dmsol) <sup>a</sup>		1.912(6) (SO <sub>4</sub> <sup>2-</sup> ) <sup>a</sup>
M–O6	2.178(7) (H <sub>2</sub> O) <sup>a</sup>	2.071(5) (H <sub>2</sub> O) <sup>a</sup>	2.199(4) (dmf) <sup>a</sup>	2.231(5) (dmf) <sup>a</sup>		2.022(7) (dmf) <sup>a</sup>
O–Mn–O ( <i>cis</i> )	80.4(2)–111.2(3)	86.3(3)–95.2(3)	80.99(14)–95.7(2)	80.6(2)–111.1(2)	79.6(1)–102.0(2)	86.4(3)–93.6(3)
O–M–O ( <i>trans</i> )	166.4(3); 167.6(3)	177.2(2); 177.4(2)	167.70(10); 167.75(16)	166.90(17); 167.29(17)	159.85(19); 168.82(17)	174.0(3); 175.5(3)
O <sub>sol</sub> –M–O <sub>sol</sub>	172.5(3)	177.4(3)	172.1(2)	174.68(19)	85.0(2)	178.4(3)
M···M	6.806	6.901	6.604	6.939	8.212	6.201
S···S	8.381	8.073	8.457	8.444	8.120	8.287
Angle between thiadiazole rings	0	0	0	0	24.9	0
Angle between acac–S and thiadiazole ring planes	104.6; 94.2	84.3; 83.1	80.3; 82.6	97.7; 100.5	96.0; 99.0	92.4; 89.9

<sup>a</sup> The oxygen atom belongs to that solvent molecule. Symmetry code: A: **1**:  $x + 2, -y + 2, -z + 2$ ; **2**:  $-x + 2, -y + 2, -z + 2$ ; **3**:  $-x + 1, -y + 2, -z + 1$ ; **4**:  $-x, -y + 1, -z$ ; **5**:  $-x, y, -z + 1/2$ ; **6**:  $-x + 1, -y + 1, -z$ .

In contrast with the *trans*-manner coordination of the solvent ligands in **1–4**, both the H<sub>2</sub>O molecules are in a *cis*-manner in the aqua dimanganese macrocycle [MnL(H<sub>2</sub>O)<sub>2</sub>] (**5**) (Fig. 5). Complex **5** with  $Z = 4$  in space group *Ccca* has crystallographically imposed 222-symmetry. The molecular structure possesses the highest C<sub>2h</sub> symmetry among all the mentioned dimetal macrocycles, though its coordination sphere of the Mn(II) ion has a substantial distortion from octahedral geometry. The acac in the enol-form chelates to the Mn ion forming non-planar six-membered chelate rings. The dihedral angle between both planes (O1–Mn–O2 and O1A–Mn–O2A) is 78.5° and is obviously larger than those in **1–4**, giving rise to a larger Mn···MnA separation of 8.210 Å, while the S2···S2A separation of 8.120 Å is comparable to those in other dimetal macrocyclic complexes. Both the thiadiazole rings in **5** are inclined to each other with an angle of 25.8°. It is considered that all the differences in structure should stem from the two small H<sub>2</sub>O ligands which coordinate to the Mn ion in *cis*-manner. Otherwise, dmf or dmsol ligands preferably coordinate to the octahedral metal ion in *trans*-manner owing to steric factors.

**Fig. 5** Structure of **5** showing thermal ellipsoids at 30% probability. Two H<sub>2</sub>O molecules are enclosed (symmetry mode: A:  $-x, y, -z + 1/2$ ; B:  $x, -y + 3/2, -z + 5/2$ ).

Diiron complexes **6**, **7** and **8** can also be considered as 24-membered macrocyclic complexes though a sulfate anion bridges between both the Fe(III) ions, dividing the macrocycle into two parts. In the structure of **8** the central sulfate moiety is disordered about the inversion centre. The structural parameters of **8** are listed in Table 1, showing shorter metal–O distances than those in the Mn and Ni analogues. The sulfate ion exists inside the macrocycle and coordinates to both the Fe(III) ions by symmetrically related O5 and O5A as shown in Fig. 6. A rough structure of **7** is shown in Fig. S7, ESI.† The sulfate bridge shortens the separation of Fe···FeA to 6.201 Å, the shortest metal···metal separation among all the dimetal macrocycles, while the S2···S2A separation of 8.287 Å is comparable to those of other dimetal (Mn, Ni) macrocycles. Meanwhile bond valence sum (BVS) analysis<sup>25</sup> has been performed to calculate the oxidation state of the metal centre.

**Fig. 6** Structure of **8** showing thermal ellipsoids at 30% probability. A sulfate ion inside the macrocycle coordinates to both the Fe(III) ions. The solvate CH<sub>2</sub>Cl<sub>2</sub> molecules are outside the macrocycle and omitted for clarity (symmetry code: A:  $-x + 1, -y + 1, -z$ ).

The bond valences ( $s$ ) were calculated according to the following equation,

$$s = \exp[(r_0 - r)/B]$$

where  $r$  is the observed Fe–O bond length and  $r_0$  and  $B$  are empirically determined parameters. This calculation gave a BVS value of 3.3+ for complex **8**, supporting the Fe(III) oxidation state. There are three types of Fe–O distances, Fe–O<sub>acac</sub> (1.968(6)–1.986(6) Å), Fe–O<sub>dmf</sub> (2.022(7) Å) and Fe–O<sub>SO<sub>4</sub></sub> (1.912(6) Å). These Fe–O bond lengths are consistent with those of other Fe<sup>III</sup>(acac) complexes<sup>26</sup> (1.97–2.02 Å) and shorter than those of Fe<sup>II</sup>(acac) complexes<sup>27</sup> reported (2.00–2.33 Å).

The size of host cavity is estimated by M...MA (6.20–8.21 Å) and S2...S2A (8.07–8.46 Å) separations for these macrocycles. These host cavities of sufficiently large size allow the solvent molecules to exist inside the macrocycle as the guest molecules. Two H<sub>2</sub>O molecules are enclosed in the cavity of **5** and one sulfate anion in **7** and **8**. Hydrogen bonding interactions were observed between the solvent molecules in the cavity. In the structure of **2** two dmf molecules are hydrogen-bonded to the aqua ligand with an O6...O7 separation of 2.728(7) and 2.796(8) Å. Also, hydrogen bonds were found between the H<sub>2</sub>O ligand and neighboring solvate H<sub>2</sub>O molecules (O<sub>H<sub>2</sub>O</sub>...O<sub>H<sub>2</sub>O</sub> 2.703 Å) in **5**, as well as between the H<sub>2</sub>O and carbonyl O atom (O<sub>H<sub>2</sub>O</sub>...O<sub>carbonyl</sub> 2.835 Å). In addition, the solvate H<sub>2</sub>O molecule is hydrogen-bonded to the N atom of thiadiazole ring with an N...O<sub>H<sub>2</sub>O</sub> separation of 2.924 Å. A packing diagram of **5** (Fig. 7) shows these H<sub>2</sub>O molecules existing in the channels formed by the overlapping cavities. Similar

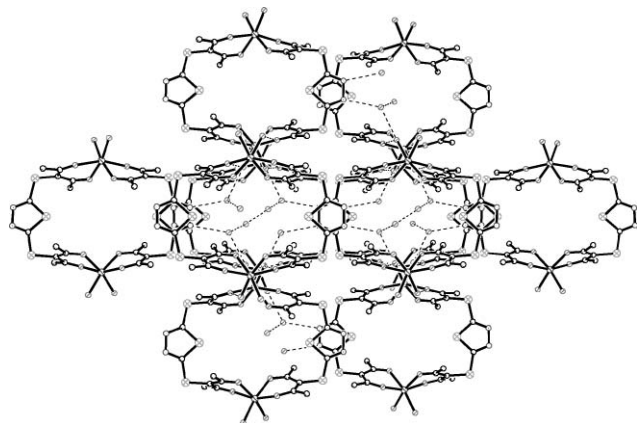


**Fig. 7** Packing diagram of **5**. Solvate and ligated H<sub>2</sub>O molecules exist in the channels formed by the overlapping cavities. Hydrogen bonding interactions are shown as dotted lines.

channels and the trapped solvent molecules were also found in other compounds (see Fig. S4, ESI†). Interestingly, the adjacent thiadiazole rings overlap in a parallel manner in a head-to-tail manner with a face-to-face distance of 3.54 Å, indicating  $\pi$ - $\pi$  stacking interactions.

### Infrared spectra and the trapped molecules

IR spectra display characteristic features of the coordinated H<sub>2</sub>L ligand and the trapped solvent molecules. In Table 2 the relevant absorptions for these complexes are listed and the empirical assignments are given. Typical absorptions of the 24-membered dimetal macrocyclic complexes are three strong peaks between 1591 and 1333 cm<sup>-1</sup> assignable to C=O and C=N bonds of the L ligand. Complexes **2–4** containing ligated and solvate dmf molecules show the C=O vibrations as sharp signals at 1674–1649 cm<sup>-1</sup>. The coordinated and solvate H<sub>2</sub>O molecules were easily assigned to the broad peaks at 3419–3373 cm<sup>-1</sup> with medium intensity for the complexes containing aqua molecules. Free dmsO has a strong absorption at 1055 cm<sup>-1</sup>. However the dmsO ligand coordinates to the metal giving rise to a weakening of the S=O bond and red shift of the infrared frequency. It should be noted that the peaks of dmsO are coincident with several peaks (1060(s) and 1022(m) cm<sup>-1</sup>) of the free H<sub>2</sub>L and they thus overlap each other. The spectra of complexes **1**, **4** and **6** exhibit relevant strong absorptions in this area as follows: 1053(m), 1026(s) cm<sup>-1</sup> for **1**; 1014(s) cm<sup>-1</sup> for **4**; 1020(s) cm<sup>-1</sup> for **6**. These absorptions should contain the contribution of the dmsO ligands since the peaks in the region 1026–1014 cm<sup>-1</sup> are obviously enhanced. An uncoordinated SO<sub>4</sub><sup>2-</sup> group with T<sub>d</sub> symmetry has infrared active  $\nu_3$  and  $\nu_4$  fundamentals at 1104 and 613 cm<sup>-1</sup>.<sup>28</sup> If the sulfate coordinates to a metal ion in a bidentate and/or bridged mode, the spectra will undergo marked change<sup>28</sup> with the lowering of the symmetry of the sulfate ion, the  $\nu_1$  fundamental will appear with medium intensity, and moreover, the  $\nu_3$  and  $\nu_4$  will split.<sup>29</sup> In di-Fe(III) macrocyclic complexes the sulfate acts as a bidentate bridged ligand and its absorption bands in the sulfate region are shown in Table 3, exhibiting several split peaks, such as 1225, 1128, 1065 cm<sup>-1</sup> and 1221, 1126, 1065 cm<sup>-1</sup> for **6** and **7**, respectively. This spectral feature is consistent with the fact reported in refs. 28–30 that the free sulfate peaks at 1104 cm<sup>-1</sup> undergo splitting into three bands.

### Thermal analyses

The thermal stability of the macrocyclic complexes has been examined by thermogravimetric analyses. The TGA curves were

**Table 2** Relevant infrared data (cm<sup>-1</sup>) for dimetal macrocyclic compounds and ligand H<sub>2</sub>L

	$\nu(\text{H}_2\text{O})$	$\nu(\text{C}=\text{O})_{\text{dmf}}$	$\nu(\text{C}=\text{O}, \text{C}=\text{N})_{\text{L}}$	$\nu(\text{S}=\text{O})_{\text{dmsO}}$	$\nu(\mu\text{-SO}_4^{2-})$		
					$\nu_1$	$\nu_3$	$\nu_4$
H <sub>2</sub> L			1549, 1390				
[MnL(H <sub>2</sub> O)(dmsO)] <sub>2</sub> ·2dmsO ( <b>1</b> )	3419		1587, 1383, 1336	1053, 1026			
[NiL(H <sub>2</sub> O)(dmf)] <sub>2</sub> ·2dmf ( <b>2</b> )	3400	1674, 1649	1587, 1383, 1336				
[MnL(dmf) <sub>2</sub> ] ( <b>3</b> )		1676, 1653	1589, 1373, 1336				
[MnL(dmf)(dmsO)] <sub>2</sub> ( <b>4</b> )		1660	1591, 1383, 1335	1014			
[MnL(H <sub>2</sub> O) <sub>2</sub> ]·6H <sub>2</sub> O ( <b>5</b> )	3400		1578, 1375, 1333				
[Fe <sub>2</sub> L <sub>2</sub> (dmsO) <sub>2</sub> (SO <sub>4</sub> )]·2H <sub>2</sub> O ( <b>6</b> )	3394		1566, 1367, 1338	1020	980	1225, 1128, 1065	667, 619, 600
[Fe <sub>2</sub> L <sub>2</sub> (H <sub>2</sub> O) <sub>2</sub> (SO <sub>4</sub> )]·2H <sub>2</sub> O ( <b>7</b> )	3373		1564, 1365, 1338		985	1221, 1126, 1065	652

Table 3 Crystallographic data for 24-membered dimetal macrocyclic complexes and ligand H<sub>2</sub>L

Compound	1	2	3	4	5	8	H <sub>2</sub> L
Formula	C <sub>33</sub> H <sub>42</sub> Mn <sub>2</sub> N <sub>4</sub> O <sub>14</sub> S <sub>10</sub>	C <sub>34</sub> H <sub>46</sub> Ni <sub>2</sub> N <sub>8</sub> O <sub>14</sub> S <sub>6</sub>	C <sub>36</sub> H <sub>52</sub> Mn <sub>2</sub> N <sub>8</sub> O <sub>12</sub> S <sub>6</sub>	C <sub>34</sub> H <sub>46</sub> Mn <sub>2</sub> N <sub>6</sub> O <sub>12</sub> S <sub>8</sub>	C <sub>32</sub> H <sub>44</sub> Mn <sub>2</sub> N <sub>4</sub> O <sub>18</sub> S <sub>6</sub>	C <sub>33</sub> H <sub>42</sub> Cl <sub>4</sub> Fe <sub>2</sub> N <sub>6</sub> O <sub>14</sub> S <sub>7</sub>	C <sub>12</sub> H <sub>14</sub> Ni <sub>2</sub> O <sub>4</sub> S <sub>3</sub>
<i>M</i>	1147.26	1134.67	1091.10	1101.16	978.87	1212.64	346.43
$\lambda$ (Mo-K $\alpha$ )	0.71073	0.71073	0.71073	0.71073	0.71073	0.71073	0.71073
<i>T</i> /°C	20	20	20	20	20	20	20
Space group	P $\bar{1}$	P $\bar{1}$	P $\bar{1}$	P $\bar{1}$	<i>Ccca</i>	<i>P2<sub>1</sub>/c</i>	<i>P2<sub>1</sub>/n</i>
<i>a</i> /Å	10.0088(8)	10.5249(14)	11.0902(8)	10.8989(1)	18.5969(7)	11.4902(8)	12.9134(2)
<i>b</i> /Å	11.3527(9)	11.7042(15)	11.2049(7)	11.0697(3)	22.4917(7)	15.0401(9)	8.7061(3)
<i>c</i> /Å	11.9496(9)	12.1680(15)	11.9250(8)	11.7666(3)	10.3271(4)	15.0968(9)	13.7625(5)
<i>a</i> /°	69.390(2)	98.875(2)	111.575(1)	107.710(1)			
$\beta$ /°	81.425(2)	105.571(2)	107.820(1)	109.114(1)			
$\gamma$ /°	84.084(2)	107.445(2)	96.066(1)	99.806(1)			
<i>V</i> /Å <sup>3</sup>	1254.83(17)	1331.8(3)	1271.4(2)	1218.97(5)	4319.6(3)	102.810(2)	95.259(2)
<i>Z</i>	1	1	1	1	4	2	4
<i>D<sub>c</sub></i> /g cm <sup>-3</sup>	1.518	1.415	1.425	1.500	1.505	1.583	1.493
$\mu$ /mm <sup>-1</sup>	0.980	1.006	0.804	0.921	0.944	1.131	0.496
<i>R<sup>a</sup></i>	0.1064	0.0809	0.0771	0.0751	0.0515	0.0948	0.0556
<i>R<sub>w</sub><sup>b</sup></i>	0.1893	0.1467	0.1406	0.1441	0.1342	0.2475	0.1085

<sup>a</sup>  $R = \sum ||F_o| - |F_c|| / \sum (|F_o| + |F_c|)$ ; <sup>b</sup>  $R_w = [\sum w(F_o - F_c)^2 / \sum w(F_o^2 + F_c^2)]^{1/2}$ ;  $w = 1/[\sigma^2(F_o^2) + (0.0000P)^2 + 12.2738P]$  for **1**;  $w = 1/[\sigma^2(F_o^2) + (0.0369P)^2 + (0.0369P)^2 + (0.0127P)^2 + (0.0000P)^2 + 3.1399P]$  for **3**;  $w = 1/[\sigma^2(F_o^2) + (0.0232P)^2 + 4.8641P]$  for **4**;  $w = 1/[\sigma^2(F_o^2) + (0.0770P)^2 + 9.3548P]$  for **5**;  $w = 1/[\sigma^2(F_o^2) + (0.1690P)^2 + 6.3786P]$  for **8**;  $w = 1/[\sigma^2(F_o^2) + (0.0127P)^2 + 2.6752P]$  for H<sub>2</sub>L;  $P = (F_o^2 + 2F_c^2)/3$ .

determined in nitrogen atmosphere in the range from 25 to 1200 °C. Free H<sub>2</sub>L showed relatively high thermal stability with an insignificant weight loss (0.21%) before 188 °C (ESI,†Fig. S8 and S9). Then rapid decomposition occurred accompanying a weight loss of >50% (188–225 °C). It is expected that the L ligand in these complexes should have thermal stability below 180 °C. The TGA and DTA curves (Fig. 8) of di-Mn complex **3** showed a first weight loss of 26.4% (177–242 °C) with an endothermic peak corresponding to the release of all the four dmf molecules (calc. 26.8%). With increasing of the temperature to 321 °C the collapse of the macrocyclic backbone led to a further weight loss of 50%. Di-Ni complex **2** showed similar thermal behavior (ESI,†Fig. S10) including a first weight loss of *ca.* 4.7% (below 101 °C) corresponding to the release of two trapped water molecules (calc. 3.17%), and a weight loss of 29.2% (below 272 °C) attributed to the removal of solvate and coordinated solvent molecules (calc. 2H<sub>2</sub>O, 3.17%; 4dmf, 25.77%). Then a rapid weight loss (*ca.* 65%) was observed from 272 to 400 °C accompanying the collapse of the macrocyclic backbone. Complex **5** was observed to have a weight loss of 18.48% from 150 to 241 °C (ESI,† Fig. S12) which is consistent with its release of the solvate and ligated H<sub>2</sub>O molecules (calc. 10H<sub>2</sub>O, 18.40%). Rapid weight loss was observed at >241 °C indicating the collapse of the backbone. The thermogravimetric analyses have displayed the desolvation and decomposition processes of the complexes. However, the final products after continuing heating were unidentified under dinitrogen atmosphere. As a comparison, the TGA curves were determined in air in the range from 25 to 700 °C in order to observe the oxidation reaction in the participation of dioxygen. The thermogravimetric analyses of these complexes display occurrence of three consecutive processes: desolvation, decomposition/oxidation of the ligand and inorganic residue formation. Complex **2** lost its coordination water molecules at 104 °C and its dmf molecules at 213 °C with the expected endothermic peaks (Figure S11). The subsequent decomposition and oxidation were in the range 270–480 °C and 480–530 °C with two strong exothermic peaks and drastic weight loss. The final residue in the temperature range 530–700 °C remained constant weight (11.92%) and could be considered as the metal oxide NiO (calc. 13.1%) Similar thermal behaviors for di-Mn complexes **4** and **5** in air atmosphere were observed (ESI,†Fig. S13 and S14). The final residue of the di-Mn complexes with constant weight

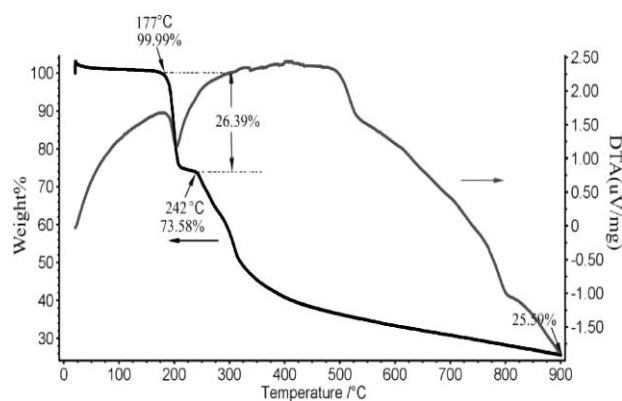
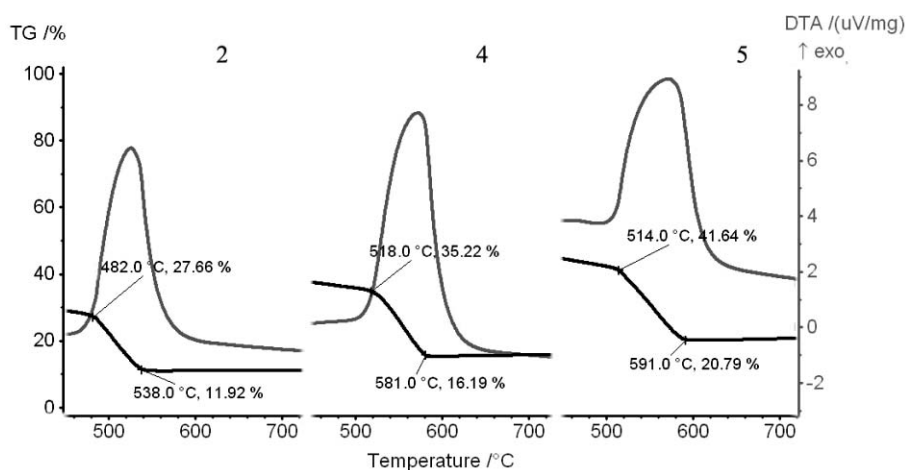


Fig. 8 DTA and TG curves determined under dinitrogen atmosphere for [MnL(dmf)<sub>4</sub>].



**Fig. 9** DTA and TG curves determined under air atmosphere for **2**, **4** and **5** in the temperature range 450–700 °C. A common exothermic peak was observed.

(**4**, 16.2%; **5**, 20.8%) at 580–700 °C was tentatively considered as  $\text{MnO}_2$  when compared to calculated values (**4**, 15.8%; **5**, 18.8%). Interestingly a similar weight loss (Fig. 9) has been found for these macrocycle complexes in the temperature range 500–600 °C with a strong exothermic reaction. It may stem from a common thermal behavior, in which a metal sulfate formed in the decomposition of the macrocyclic backbone at 300–500 °C. This has been supported by the weight loss values. The thermal decomposition/oxidation of the macrocycle appears to produce  $\text{Mn}_2(\text{SO}_4)_3$  with 64.78% (calc. 63.86%) or 58.36% (calc. 56.97%) weight loss, respectively, for **4** and **5**, and  $\text{NiSO}_4$  with 72.34% (calc. 72.68%) weight loss for di-Ni complex **2**. These sulfates were further oxidized to result in the metal oxide  $\text{MnO}_2$  or  $\text{NiO}$  after continuing heating.

## Conclusions

(1) 2,5-Di(3-pentanedionylthio)-1,3,4-thiadiazole ( $\text{H}_2\text{L}$ ) has been used to synthesize new 24-membered dimetal (Mn(II), Ni(II) and Fe(III)) macrocycle complexes. The reaction of  $\text{H}_2\text{L}$  with either  $\text{Mn}(\text{OAc})_2$  or  $\text{Mn}(\text{Hacac})_3$  produces only di-Mn(II) macrocycles, while the reaction with  $\text{FeSO}_4$  affords di-Fe(III) macrocycles in which a sulfate ion bridges between both the Fe(III) ions.

(2) C–H bond activation and C–S bond formation have been observed in an aerobic assembly system of  $\text{MnCl}_2$ , dipotassium 1,3,4-thiadiazole-2,5-dithiolate ( $\text{K}_2\text{tdadt}$ ) and acetylacetonate ( $\text{H}_2\text{acac}$ ) in various solvents, leading to the di-Mn(II) macrocycle complexes. The participation of the manganese ion is essential for the C–S bond fusion. Disulfide has been considered as a possible intermediate. A similar assembly using 2-mercaptobenzimidazole has led to an organic compound 2-(3-pentanedionylthio)benzimidazole.

(3) The 24-membered dimetal macrocycle complexes provide a host cavity correlating to the molecular recognition. The solvents (dmsO, dmf and  $\text{H}_2\text{O}$ ) and the sulfate ion are trapped inside the cavity and have been assigned by IR spectra. Meanwhile, the thermogravimetric analyses of these complexes show the occurrence of three consecutive processes: desolvation, decomposition/oxidation of the ligand and inorganic residue formation, indicating the thermal stability of the macrocycle backbone when the temperature is below 240 °C. The thermal behavior

between 80 and 240 °C mainly correlated to the trapped solvent molecules.

## Experimental

All manipulations were performed under aerobic conditions with materials as received. IR spectra were recorded on a Magna-75-FT-IR spectrophotometer as KBr pellets (4000–400  $\text{cm}^{-1}$ ). The  $^1\text{H}$  NMR spectra were recorded on a Bruker-Am 500 spectrometer with TMS as standard. Thermal analysis was performed on NETZSCH STA449C thermogravimetric instrument. Elemental analyses were performed using a Germany Elemental Analyzer Vario EL III.

### 2,5-Di(3-pentanedionylthio)-1,3,4-thiadiazole ( $\text{H}_2\text{L}$ )

Dipotassium 1,3,4-thiadiazole-2,5-dithiolate ( $\text{K}_2\text{tdadt}$ , 2.26 g, 10 mmol) was dissolved in 50 mL of MeOH. To the solution 2.69 g (20 mmol) of ClHacac was added and stirred for 6 h. After filtration 3.1 g of white powder was collected in 90% yield, which was recrystallized in  $\text{CH}_2\text{Cl}_2$  to get square crystals of  $\text{H}_2\text{L}$ . Elemental analysis: calc. for  $\text{C}_{12}\text{H}_{14}\text{N}_2\text{O}_4\text{S}_3$  (%): C 41.60, H 4.07, N 8.09, S 27.77; found: C 41.38, H 3.98, N 7.95, S 27.39.  $^1\text{H}$  NMR ( $\text{CDCl}_3$ ,  $\delta$ /ppm): 2.417 (6H,  $\text{CH}_3$ ), 17.33 (1H, C=C–OH).

**[MnL( $\text{H}_2\text{O}$ )(dmsO)] $_2$ ·2dmsO (**1**).**  $\text{H}_2\text{L}$  (0.20 g, 0.5 mmol) was dissolved in 25 mL of mixed solvent ( $\text{CH}_2\text{Cl}_2$ –dmsO–MeOH, 2 : 1 : 2, v/v/v) and 0.063 g (0.5 mmol) of  $\text{Mn}(\text{OAc})_2 \cdot 4\text{H}_2\text{O}$  was added under stirring. After filtration, the slight yellow filtrate was allowed to stand for several days to deposit yellow rhombic crystals of **1** (0.18 g, yield 31%). Elemental analysis: calc. for  $\text{C}_{32}\text{H}_{52}\text{Mn}_2\text{N}_4\text{O}_{14}\text{S}_{10}$  (%): C 33.50, H 4.57, N 4.88, S 27.94, Mn 9.58; found: C 33.41, H 4.61, N 4.82, S 27.68, Mn 10.13.

**[NiL( $\text{H}_2\text{O}$ )(dmf)] $_2$ ·2dmf (**2**).** The above synthetic procedure of **1** was used for the synthesis of **2** with  $\text{Ni}(\text{NO}_3)_2 \cdot 6\text{H}_2\text{O}$  and dmf was used as the solvent. Light-blue crystals (0.10 g, yield 18%) were collected. Elemental analysis: calc. for  $\text{C}_{36}\text{H}_{56}\text{Ni}_2\text{N}_8\text{O}_{14}\text{S}_6$  (%): C 38.10, H 4.97, N 9.88, S 16.95; found: C 37.44, H 4.77, N 9.63, S 17.00.

**[MnL(dmf)<sub>2</sub>]<sub>2</sub> (3).** A solution of 0.125 g of Mn(Hacac)<sub>3</sub> (0.36 mmol) in 10 mL of dmf was added with stirring to 10 mL of CH<sub>2</sub>Cl<sub>2</sub> containing H<sub>2</sub>L (0.20 g, 0.5 mmol). The solution was stirred for 1 h and filtered. The filtrate was allowed to stand for several days to deposit yellow rhombic crystals which were collected to obtain 0.10 g of **3** (yield 51%). Elemental analysis: calc. for C<sub>36</sub>H<sub>52</sub>Mn<sub>2</sub>N<sub>8</sub>O<sub>12</sub>S<sub>6</sub> (%): C, 39.62; H, 4.80; N, 10.27; S, 17.64; found: C, 39.71; H, 4.68; N, 10.26; S, 17.45.

**[MnL(dmf)(dmsO)<sub>2</sub>]<sub>2</sub> (4).** A solution of 0.4 g (2 mmol) of MnCl<sub>2</sub>·4H<sub>2</sub>O in 10 mL of dmf–dmsO (1 : 1, v/v) was added to 15 mL of an MeOH solution containing 0.36 g (3.6 mmol) of H<sub>2</sub>acac and 0.45 g (1.99 mmol) of K<sub>2</sub>tdadt, and stirred for 12 h. The filtrate was allowed to stand for several days affording 0.21 g (yield 21%) of yellow block crystals. Elemental analysis: calc. for C<sub>34</sub>H<sub>50</sub>Mn<sub>2</sub>N<sub>6</sub>O<sub>12</sub>S<sub>8</sub> (%): C, 37.08; H, 4.58; N, 7.63; S, 23.29; Mn, 9.98; found: C, 36.58; H, 4.66; N, 7.34; S, 23.60; Mn, 10.48.

#### **[MnL(H<sub>2</sub>O)<sub>2</sub>]<sub>2</sub>·6H<sub>2</sub>O (5).**

*Method 1.* The synthetic procedure of **4** was used with a change of the solvent for MnCl<sub>2</sub>·4H<sub>2</sub>O (20 mL of H<sub>2</sub>O–MeOH, 1 : 1, v/v). Yellow rhombic crystals (0.43 g, yield 49%) were collected. Elemental analysis: calc. for C<sub>24</sub>H<sub>44</sub>Mn<sub>2</sub>N<sub>4</sub>O<sub>18</sub>S<sub>6</sub> (%): C, 29.42; H, 4.49; N, 5.72; S, 19.61; Mn, 11.24; found: C, 31.44; H, 4.66; N, 5.74; S, 19.74; Mn, 12.06. The amount of the hydrate molecules may change in the product giving rise to analysis deviation.

*Method 2.* 0.45 g (1.99 mmol) of K<sub>2</sub>tdadt was added to 20 mL of MeOH to obtain a yellow solution to which HOAc was added dropwise to adjust the pH of the reaction mixture to 6.0. To the yellow solution 0.70 g (1.99 mmol) of Mn(Hacac)<sub>3</sub> was added and the solution stirred for 2 h. After filtration the filtrate was allowed to stand for two weeks at room temperature to deposit yellow rhombic crystals which were collected to obtain 0.59 g of **5** (yield 61%).

*Parallel anaerobic experiment.* The synthetic procedure of method 1 was used but the procedure was performed under dinitrogen atmosphere. The filtrate was allowed to stand for several days accompanying the concentration of the filtrate sometimes. We failed to obtain any isolable product during two months, indicating that anaerobic conditions did not lead to complex **5**. Then exposure of the solution to air gave rise to the rapid deposition of yellow rhombic crystals which were collected in moderate yield and identified as **5** by X-ray diffraction.

**[Fe<sub>2</sub>L<sub>2</sub>(dmsO)<sub>2</sub>(SO<sub>4</sub>)]·2H<sub>2</sub>O (6).** To a solution of H<sub>2</sub>L (0.20 g, 0.5 mmol) in 10 mL of CH<sub>2</sub>Cl<sub>2</sub>, 0.14 g (0.5 mmol) of FeSO<sub>4</sub>·7H<sub>2</sub>O in 10 mL of dmsO was added under stirring. The deep red solution was filtered and the filtrate was allowed to stand for days to deposit red crystals (0.15 g, yield 56%). Elemental analysis: calc. for C<sub>28</sub>H<sub>40</sub>Fe<sub>2</sub>N<sub>4</sub>O<sub>16</sub>S<sub>9</sub> (%): C, 30.88; H, 3.70; N, 5.14; S, 26.50; found: C, 30.76; H, 3.90; N, 5.15; S, 26.21.

**[Fe<sub>2</sub>L<sub>2</sub>(H<sub>2</sub>O)<sub>2</sub>(SO<sub>4</sub>)]·3H<sub>2</sub>O (7).** The synthetic procedure of **6** was used with a change of the solvent for FeSO<sub>4</sub>·7H<sub>2</sub>O (10 mL of CH<sub>3</sub>OH). Red hexagonal crystals of [Fe<sub>2</sub>L<sub>2</sub>(H<sub>2</sub>O)<sub>2</sub>(SO<sub>4</sub>)]·3H<sub>2</sub>O (0.08 g, yield 32%) were collected. Elemental analysis: calc. for C<sub>24</sub>H<sub>34</sub>Fe<sub>2</sub>N<sub>4</sub>O<sub>17</sub>S<sub>7</sub> (%): C, 29.19; H, 3.47; Fe, 11.32; N, 5.68; S, 22.74; found: C, 28.94; H, 3.46; Fe, 11.20; N, 5.61; S, 22.70. A rough structure of complex **7** was solved (see ESI,† Fig. S7).<sup>31</sup>

**[Fe<sub>2</sub>L<sub>2</sub>(dmf)<sub>2</sub>(SO<sub>4</sub>)]·2CH<sub>2</sub>Cl<sub>2</sub> (8).** The synthetic procedure of **6** was used with a change of the solvent for FeSO<sub>4</sub>·7H<sub>2</sub>O (10 mL of dmf–dmsO, 1 : 1 v/v). A few red rhombic crystals were selected from the dark red impure powder and identified as **8** by X-ray diffraction.

**Assembly reaction of FeSO<sub>4</sub>·7H<sub>2</sub>O with K<sub>2</sub>tdadt and H<sub>2</sub>acac.** The procedure for **5** (method 1) was used with the use of FeSO<sub>4</sub>·7H<sub>2</sub>O (or FeCl<sub>2</sub>·4H<sub>2</sub>O). The filtrate was allowed to stand for several days to deposit black crystals, which were collected in moderate yield and identified as Fe(Hacac)<sub>3</sub> by X-ray diffraction, indicating that the experiment did not lead to the formation of C–S bond and the di-Fe macrocycle.

**2-(3-Pentanedionylthio)benzimidazole (HL').** To a CH<sub>3</sub>OH solution (15 mL) of 0.4 g (2 mmol) of MnCl<sub>2</sub>·4H<sub>2</sub>O and 0.36 g (3.6 mmol) of acetylacetone (H<sub>2</sub>acac), 0.30 g (2 mmol) of 2-mercaptobenzimidazole was added and stirred for 12 h. The filtrate was reduced to ca. 10 mL by volatilization at room temperature to deposit yellow needle crystals (62 mg, yield 13%). Elemental analysis: calc. for C<sub>12</sub>H<sub>12</sub>N<sub>2</sub>O<sub>2</sub>S (%): C 58.04, H 4.87, N 11.28, S 12.91; found: C 58.46, H 4.61, N 10.85, S 12.45. <sup>1</sup>H NMR (CDCl<sub>3</sub>, δ, ppm): 2.38 (6H, CH<sub>3</sub>), 7.40 (1H, NH), 7.88 (broad, 4H, CH benzene ring), 17.63 (1H, C=C–OH). The structure has been determined by X-ray diffraction and is the same to that reported in literature.<sup>32</sup>

#### **X-Ray structure determinations**

All the crystals suitable for X-ray diffraction were selected from the reaction solutions. The diffraction data were collected on a Siemens SMART CCD diffractometer with graphite-monochromated Mo-Kα radiation (λ = 0.71073 Å) using ω-scan mode at 293 K. The intensity data were corrected for Lorentz-polarization factors and empirical absorption correction was applied. The structures were solved by direct methods and Fourier techniques for each compound and refined by full-matrix least-squares calculation with the SHELXL-97 program package.<sup>33</sup> All the non-hydrogen atoms were refined anisotropically. One oxygen atom (O4) in the solvate H<sub>2</sub>O molecule for complex **5** was found to be disordered in two positions with occupancy of 0.5. For complex **8**, the sulfur atom S4 and the oxygen atoms O6 and O7 are disordered in two positions with occupancy of 0.5. Only a rough structure was solved<sup>31</sup> for complex **7** with similar features found to that of complex **8**. For all compounds, hydrogen atoms were geometrically located and added to the structure factor calculations but their positions were not refined. The crystallographic data were compiled in Table 3, in which the data of complex **7** was omitted.<sup>31</sup>

CCDC reference numbers 281993–281997 for complexes **1–5**, 281998 for **8** and 281999 for H<sub>2</sub>L.

For crystallographic data in CIF or other electronic format see DOI: 10.1039/b604579k

#### **Acknowledgements**

This work was supported by NNSFC (No. 20471061) and The Sci. & Tech. Innovation Foundation for the Young Scholar of Fujian Province (No. 2005J059).

## References

- 1 (a) M. L. Lehaire, R. Scopelliti, H. Piotrowski and K. Severin, *Angew. Chem., Int. Ed.*, 2002, **41**, 1419–1422; (b) V. L. Pecoraro, A. J. Stemmler, B. R. Gibney, J. J. Bodwin, H. Wang, J. W. Kampf and A. Barwinski, *Prog. Inorg. Chem.*, 1997, **45**, 83–177; (c) J. J. Bodwin, A. D. Cutland, R. G. Malkani and V. L. Pecoraro, *Coord. Chem. Rev.*, 2001, **216**, 489–512; (d) M. H. Keefe, K. D. Benkstein and J. T. Hupp, *Coord. Chem. Rev.*, 2002, **225**, 91–121.
- 2 N. Shan, S. J. Vickers, H. Adams, M. D. Ward and J. A. Thomas, *Angew. Chem., Int. Ed.*, 2004, **43**, 3938–3941.
- 3 Z. Weng, S. Teo, L. L. Koh and T. S. A. Hor, *Organometallics*, 2004, **23**, 3603–3609.
- 4 (a) D. Gaynor, Z. A. Starikova, S. Ostrovsky, W. Haase and K. B. Nolan, *Chem. Commun.*, 2002, 506–507; (b) M. Du, Y.-M. Guo, X.-H. Bu, J. Ribas and M. Monfort, *New J. Chem.*, 2002, **26**, 645–650.
- 5 (a) D. L. Caulder and K. N. Raymond, *Acc. Chem. Res.*, 1999, **32**, 975–982; (b) D. L. Caulder and K. N. Raymond, *J. Chem. Soc., Dalton Trans.*, 1999, 1185–1200; (c) M. Fujita, *Chem. Soc. Rev.*, 1998, **6**, 417–425; (d) S. Leininger, B. Olenyuk and P. J. Stang, *Chem. Rev.*, 2000, **100**, 853–908; (e) E. Uller, B. Demleitner, I. Bernt and R. W. Saalfrank, *Struct. Bonding (Berlin)*, 2000, **96**, 149–175.
- 6 S.-X. Liu, S. Lin, B.-Z. Lin, C.-C. Lin and J.-Q. Huang, *Angew. Chem., Int. Ed.*, 2001, **40**, 1084–1087.
- 7 Y. Chen, Q. Liu, Y. Deng, H. Zhu, C. Chen, H. Fan, D. Liao and E. Gao, *Inorg. Chem.*, 2001, **40**, 3725–3733.
- 8 R. W. Saalfrank, I. Bernt, E. Uller and F. Hampel, *Angew. Chem., Int. Ed. Engl.*, 1997, **36**, 2482–2485.
- 9 M. I. Khan, S. Tabussum and R. J. Doedens, *Chem. Commun.*, 2003, 532–533.
- 10 T. Brasey, A. Buryak, R. Scopelliti and K. Severin, *Eur. J. Inorg. Chem.*, 2004, 964–967.
- 11 P. Grosshans, A. Jouaiti, V. Bulach, J.-M. Planeix, M. W. Hosseini and N. Kyritsakas, *Eur. J. Inorg. Chem.*, 2004, 453–458.
- 12 L. Barloy, G. Malaisé, S. Ramdeehul, C. Newton, J. A. Osborn and N. Kyritsakas, *Inorg. Chem.*, 2003, **42**, 2902–2907.
- 13 B. Kwak, H. Rhee and M. S. Lah, *Polyhedron*, 2000, **19**, 1985–1994.
- 14 (a) M. Loï, M. W. Hosseini, A. Jouaiti, A. D. Cian and J. Fischer, *Eur. J. Inorg. Chem.*, 1999, 1981–1985; (b) P. Grosshans, A. Jouaiti, M. W. Hosseini, A. D. Cian and N. Kyritsakas-Gruber, *Tetrahedron Lett.*, 2003, **44**, 1457–1460.
- 15 (a) T. Clifford, A. M. Danby, P. Lightfoot, D. T. Richens and R. W. Hay, *J. Chem. Soc., Dalton Trans.*, 2001, 240–246; (b) J. R. Bradbury, J. L. Hampton, D. P. Martone and A. W. Maverick, *Inorg. Chem.*, 1989, **28**, 2392–2399; (c) Z. Atherton, D. M. L. Goodgame, S. Menzer and D. J. Williams, *Inorg. Chem.*, 1998, **37**, 849–858; (d) L. J. Childs, N. W. Alcock and M. J. Hannon, *Angew. Chem., Int. Ed.*, 2001, **40**, 1079–1081; (e) A. Jouaiti, M. Loï, M. W. Hosseini and A. D. Cian, *Chem. Commun.*, 2000, 2085–2086; (f) P. D. Beer, N. Berry, M. G. B. Drew, O. D. Fox, M. E. Padilla-Tosta and S. Patell, *Chem. Commun.*, 2001, 199–200; (g) M. Vazquez, A. Taglietti, D. Gatteschi, L. Sorace, C. Sangregorio, A. M. Gonzalez, M. Maneiro, R. M. Pedrido and M. R. Bermejo, *Chem. Commun.*, 2003, 1840–1841; (h) H. Ma, M. Allmendinger, U. Thewalt, A. Lentz, M. Klinga and B. Rieger, *Eur. J. Inorg. Chem.*, 2002, 2857–2867; (i) M. Du, X.-H. Bu, Z. Huang, S.-T. Chen, Y.-M. Guo, C. Diaz and J. Ribas, *Inorg. Chem.*, 2003, **42**, 552–559; (j) H. V. Huynh, C. Schulze-Isfort, W. W. Seidel, T. Luggner, R. Frohlich, O. Kataeva and F. E. Hahn, *Chem. Eur. J.*, 2002, **8**, 1327–1335.
- 16 (a) G. Aromi, P. Gamez, O. Roubeau, P. Carrero-Berzal, H. Kooijman, A. L. Spek, W. L. Driessen and J. Reedijk, *Eur. J. Inorg. Chem.*, 2002, 1046–1048; (b) F. M. Tabellion, S. R. Seidel, A. M. Arif and P. J. Stang, *Angew. Chem., Int. Ed.*, 2001, **40**, 1529–1532; (c) G. Aromi, P. Gamez, O. Roubeau, P. C. Berzal, H. Kooijman, A. L. Spek, W. L. Driessen and J. Reedijk, *Inorg. Chem.*, 2002, **41**, 3673–3683; (d) F. M. Tabellion, S. R. Seidel, A. M. Arif and P. J. Stang, *J. Am. Chem. Soc.*, 2001, **123**, 11982–11990.
- 17 K. Matsumoto and H. Sugiyama, *Acc. Chem. Res.*, 2002, **35**, 915–926.
- 18 P. D. Clark, S. T. E. Mesher, A. Primak and H. Yao, *Catal. Lett.*, 1997, **48**, 79–82.
- 19 (a) J. A. Bonadies, M. L. Kirk, M. S. Lah, D. P. Kessissoglou, W. E. Hatfield and V. L. Pecoraro, *Inorg. Chem.*, 1989, **28**, 2037–2044; (b) C. Chen, D. Huang, X. Zhang, F. Chen, H. Zhu, Q. Liu, C. Zhang, D. Liao, L. Li and L. Sun, *Inorg. Chem.*, 2003, **42**, 3540–3548.
- 20 (a) X. Chen, B. Kang, Y. Hu and Y. Xu, *J. Coord. Chem.*, 1993, **30**, 71–77; (b) X. Chen, H. Liu, L. Weng, L. Huang, D. Wu, X. Lei and B. Kang, *J. Coord. Chem.*, 1990, **22**, 109–114.
- 21 J. P. Collman, R. L. Marshall, W. L. Young and C. T. Jr. Sears, *J. Organomet. Chem.*, 1963, **28**, 1449–1455.
- 22 J.-K. Cheng, Z.-J. Li, Y.-B. Chen, Y.-Y. Qin, Y. Kang, Y.-H. Wen and Y.-G. Yao, *Chinese J. Struct. Chem.*, 2003, **22**, 43–46.
- 23 N. W. Alcock and M. Pennington, *Acta Crystallogr., Sect. C*, 1990, **46**, 18–21.
- 24 C. Janiak, *J. Chem. Soc., Dalton Trans.*, 2000, 3885–3896.
- 25 (a) H. H. Thorp, *Inorg. Chem.*, 1992, **31**, 1585–1588; (b) I. D. Brown and D. Altermatt, *Acta Crystallogr., Sect. B*, 1985, **41**, 244–247.
- 26 (a) B. Chiari, O. Piovesana, T. Tarantelli and P. F. Zanazzi, *Inorg. Chem.*, 1984, **23**, 3398–3404; (b) L. Pang, E. A. C. Lucken and G. Bernardinelli, *J. Am. Chem. Soc.*, 1990, **112**, 8754–8764.
- 27 S. Shibata, S. Onuma, A. Iwase and H. Inoue, *Inorg. Chim. Acta*, 1977, **25**, 33–39.
- 28 K. Nakamoto, J. Fujita, S. Tanaka and M. Kobayashi, *J. Am. Chem. Soc.*, 1957, **79**, 4904–4908.
- 29 N. Nakamoto, *Infrared and Raman Spectra of Inorganic and Coordination Compounds, Part B. Applications in Coordination, Organometallic, and Bioinorganic Chemistry*, John Wiley & Sons, New York, 5th edn, 1997, pp. 79–82.
- 30 W. K. Miller, J. D. Gilbertson, C. Leiva-Paredes, P. R. Bernatis, T. J. R. Weakley, D. K. Lyon and D. R. Tyler, *Inorg. Chem.*, 2002, **41**, 5453–5465.
- 31 *Crystallographic data for 7*: C<sub>24</sub>H<sub>34</sub>Fe<sub>2</sub>N<sub>4</sub>O<sub>17</sub>S<sub>7</sub>, *M<sub>r</sub>* = 986.67, monoclinic, space group *P2<sub>1</sub>/n*, *a* = 12.1447(3), *b* = 10.9276(3), *c* = 16.555(1) Å, β = 103.085(1)°, *V* = 2139.97(8) Å<sup>3</sup>, *Z* = 2, μ = 1.087 mm<sup>-1</sup>, *R* = 0.1188 and *R<sub>w</sub>* = 0.2493 for 3209 reflections (*I* > 2σ(*I*)). Fe–O<sub>acac</sub>, 1.960(7)–1.995(8) Å; Fe–O<sub>H<sub>2</sub>O</sub>, 2.054(8) Å.
- 32 L. Smrčok, D. Tunega, V. Langer and M. Koós, *Z. Kristallogr.*, 2002, **217**, 217–222.
- 33 G. M. Sheldrick *SHELXTL-97*, Universität Göttingen, 1997.